ACS APPLIED MATERIALS & INTERFACES

Research Article

www.acsami.org

Underwater Superoleophilic to Superoleophobic Wetting Control on the Nanostructured Copper Substrates

Zhongjun Cheng,[‡] Hua Lai,[‡] Ying Du,[‡] Kewei Fu,[‡] Rui Hou,[‡] Naiqing Zhang,*[,†,‡] and Kening Sun*[,†,‡]

[†]State Key Laboratory of Urban Water Resource and Environment, School of Municipal and Environmental Engineering, Harbin Institute of Technology, Harbin, Heilongjiang 150090, P. R. China

[‡]Natural Science Research Center, Academy of Fundamental and Interdisciplinary Sciences, Harbin Institute of Technology, Harbin, Heilongjiang 150090, P. R. China

Supporting Information

ABSTRACT: Surfaces with controlled underwater oil wettability would offer great promise in the design and fabrication of novel materials for advanced applications. Herein, we propose a new approach based on self-assembly of mixed thiols (containing both $HS(CH_2)_9CH_3$ and $HS(CH_2)_{11}OH$) on nanostructured copper substrates for the fabrication of surfaces with controlled underwater oil wettability. By simply changing the concentration of $HS(CH_2)_{11}OH$ in the solution, surfaces with controlled oil wettability from the underwater superoleophilicity to superoleophobicity can be achieved. The tunable effect can be due to the synergistic effect of the surface chemistry variation and the nanostructures on the surfaces. Noticeably, the amplified effect of the nanostructures can provide better control of the underwater oil wettability between the two extremes: superoleophilicity and superoleophobicity. Moreover, we also extended the strategy to the copper mesh substrates and realized the selective oil/water separation on the as-prepared copper mesh films. This report offers a flexible approach of fabricating surfaces with controlled oil wettability, which can be further applied to other ordinary materials, and open up new perspectives in manipulation of the surface oil wettability in water.

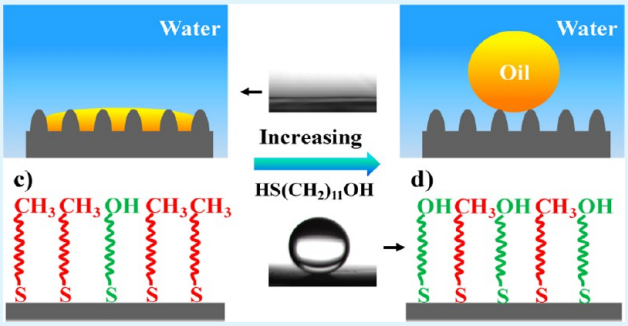

KEYWORDS: *underwater superoleophilic, superoleophobic, nanostructures, oil/water separation*

INTRODUCTION

It is well-known that fishes can swim freely under water and keep their scales clean even in the oil-polluted water when the accident of oil spill was happened. Recently, Jiang et al. revealed that the special ability of fish's scales is ascribed to underwater superoleophobicity of the surface, which arises from the combined effect of the hierarchical structures and hydrophilic chemistry of the fish scales.[1] Inspired by these findings, lots of underwater superoleophobic materials have been prepared.[2−8] These novel materials can possibly be used in lots of applications, such as bioadhesion,[9−11] microfluidic technology,[12−14] and oil/water separation.[15,16] On the other hand, underwater superoleophilic materials are also important and have also aroused much attention.[17−29] For example, Jin et al. fabricated a novel 3D network structured organosilane surface that can successfully be used in oil capture from water.[17] Considering the different oil wettabilities would endow the surfaces with different applications, it is anticipated that surfaces with controlled oil wettability would offer great promise in the design and fabrication of novel materials for real applications. Although dramatic efforts have been expended on the control of the underwater oil/solid wettability,[30−37] most works can realize only limited transition between superoleophobicity and general oleophobicity.[30] Developing a constructive strategy for the realization of the controllable underwater oil/solid wettability between the two extremes—from superoleophilicity to superoleophobicity—is still a challenge.

Herein, we provide a new approach for the fabrication of surfaces with tunable underwater oil wettability from superoleophilicity to superoleophobicity. The surfaces were prepared through combining the special nanostructures on the copper foils with modification of thiols molecules (containing $HS(CH_2)_9CH_3$ and $HS(CH_2)_{11}OH$). It is revealed that enhanced effect of the nanostructures for both oleophilic and oleophobic performances can provide better control of the oil wettability on the surface. In detail, the nanostructured $Cu(OH)_2$ was prepared first on copper foils and used as substrates, and then these substrates were modified with mixed thiols to endow the substrates with controlled surface chemistry. By simply increasing the concentration of $HS(CH_2)_{11}OH$ in the mixed solution, surfaces with finely controlled oil wettability from the underwater superoleophilicity to superoleophobicity can be achieved. The tunable effect can be attributed to the synergistic effect of the surface

Received: August 26, 2013
Accepted: October 1, 2013
Published: October 1, 2013

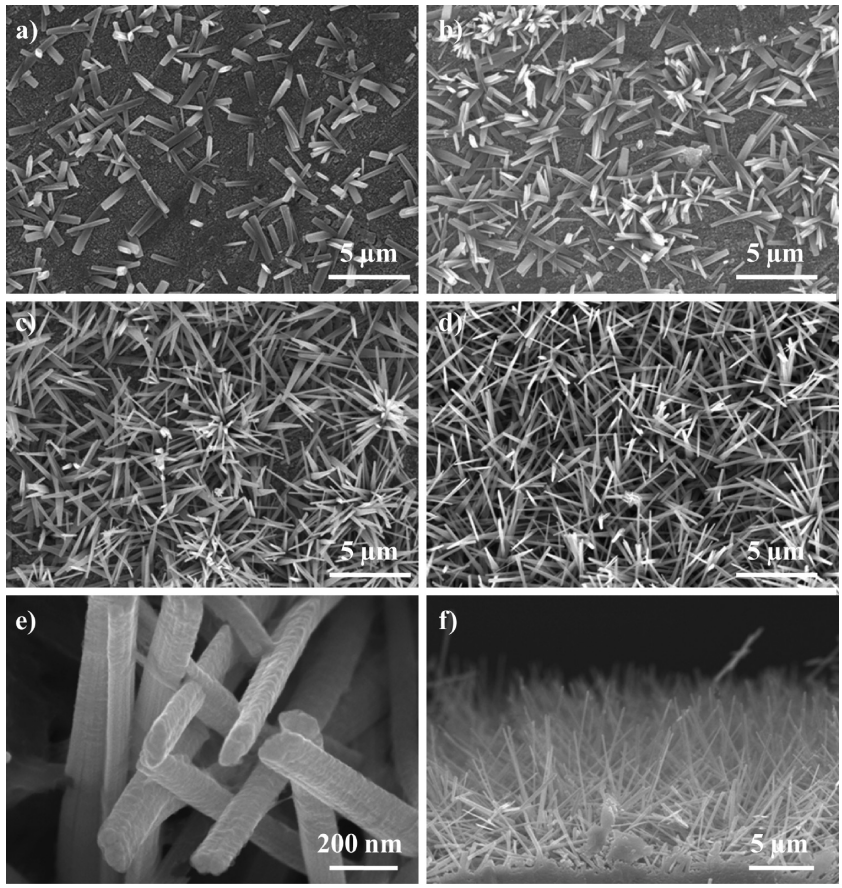

Figure 1. SEM images of the copper substrates after being immersed in the solution containing NaOH and $(NH_4)_2S_2O_8$ for different times: (a) 60 s, (b) 120 s, (c) 180 s, (d) 300 s. It can be seen that more and more nanorods would be produced as the immersion time is increased and when the time is about 300 s, the surface would be covered by the nanorods completed. (e) Magnified image of d, and (f) one can find that the diameters of the nanorods are in the range 80−150 nm and the length is about 12 μm.

chemistry variation and the nanostructures on the surfaces. Moreover, the strategy was also extended to the copper mesh substrates, the ability of controlled oil wettability allow us demonstrate a proof of selective oil/water separation via the obtained copper mesh films.

EXPERIMENTAL SECTION

Materials. $HS(CH_2)_9CH_3$, $HS(CH_2)_{11}OH$, polydimethylsiloxane (silicon oil) (Aldrich, Germany), $(NH_4)_2S_2O_8$, 1,2-dichloroethane, NaOH, ethanol, chloroform, petroleum ether, n-hexane, oil red (sudan III), methylene blue, copper mesh substrate, and copper foils, (99.9%) were obtained from Shanghai Chemical Reagent Co., China. Ultrapure water was used directly from the Milli-Q system (>1.82 MΩ cm).

Preparation of $Cu(OH)_2$ Nanorods on the Copper Substrates. The $Cu(OH)_2$ nanorods on the copper foil was fabricated by a similar method as reported.[38,39] Briefly, the copper foils were ultrasonically cleaned with acetone, ethanol, and deionized water and then immersed into a solution of $(NH_4)_2S_2O_8$ (0.1M) and NaOH (2.5M) for a certain time. After that, these copper foils were taken out, washed with abundant deionized water, and dried under N_2. The nanostructured copper mesh films were prepared with the same process.

Modification of the Nanostructured Copper Substrates. The copper foils with $Cu(OH)_2$ nanorods were first covered with a gold layer using a sputter-coater (Leica EM, SCD500), after that, these copper foils were immersed into the ethanol solution contaning $HS(CH_2)_{11}OH$ and $HS(CH_2)_9CH_3$ for about 12 h as reported.[51] The mole fraction of the $HS(CH_2)_{11}OH$ (X_{OH}) was increased from 0 to 1, and the total concentration of the two thiols molecules in the ethanol soultion was kept constant at 1 mmol L^{-1}. At last, these substrates were taken out from the solution, washed with abundant ethanol, and dried under N_2. The copper mesh films and flat copper surfaces were modified through the same process.

Oil/Water Separation Experiment. The obtained copper mesh film was fixed between two glass tubes, the oil/water mixture (about 10 mL of petroleum ether and 10 mL of water were mixed through a shake process) were poured into the upper glass tube. The photos were recorded on a camera (Canon HF M41).

Instrumentation and Characterization. The SEM images of the copper surfaces were obtained from a field-emission scanning electron microscope (HITACHI, SU8010). The oil contact angles and sliding angles were examined using a JC 2000D5 (provided by Shanghai Zhongchen Digital Technology Apparatus Co., Ltd). Before examination, the samples were placed in a cubic and transparent quartzose container filled with ultrapure water. Oil droplets with higher density than water (1, 2-dichloroethane and chloroform) were directly placed onto the surfaces carefully. For oils with low density than water (silicon oil and hexane), the surfaces were first fixed upside in the container, and then an inverted needle was used to place the oil droplet under the surface. The volume of the test oil droplet is 4 μL. The final contact angle values were attained by averaging at least five results at different positions on the same surface. Before the examination of sliding angles, a 4 μL oil droplet was first dropped on the surface, then tilted the surface until the oil droplet started to roll. X-ray photoelectron spectroscopy (XPS) data were attained with a K-Alpha electron spectrometer from Thermo Fisher Scientific Company using Al Ka (1486.6 eV) radiation. The binding energy data were calibrated referenced to the C1s line at 284.8 eV.

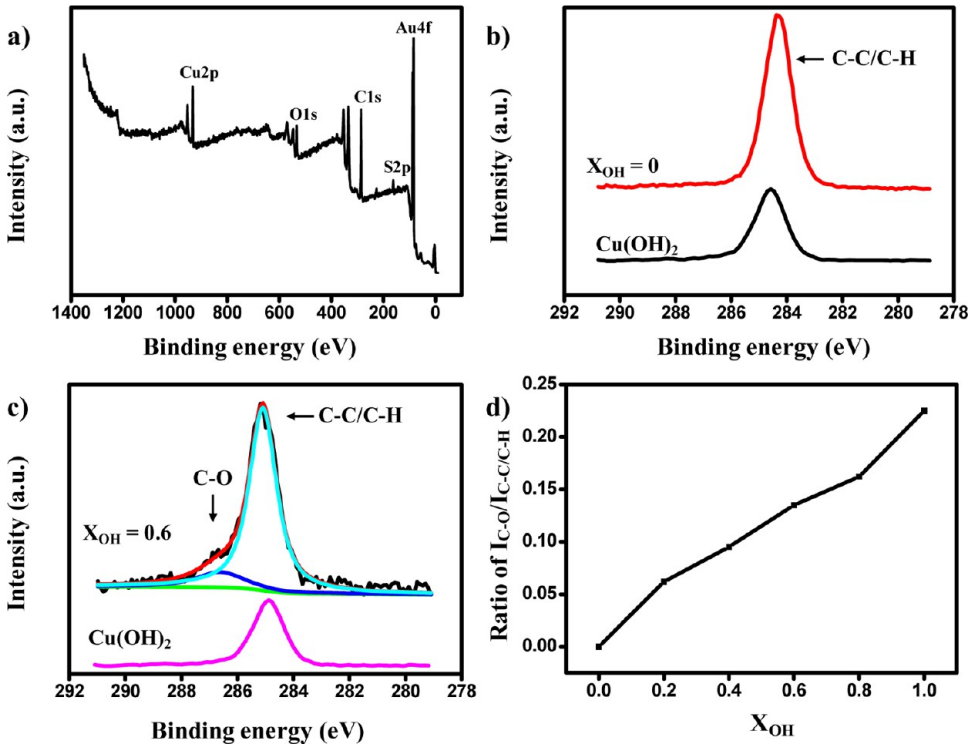

Figure 2. (a) XPS survey spectrum of the surface prepared with X_{OH} = 0.6, (b, c) high-resolution C 1s XPS spectra of the initial $Cu(OH)_2$ and the surfaces prepared with X_{OH} = 0 and X_{OH} = 0.6, respectively, (d) dependence of the ratio of $I_{C-O}/I_{C-C/C-H}$ on the X_{OH}.

RESULTS AND DISCUSSION

As is known, surface wettability is controlled by both the surface chemical composition and the microstructures.[40−48] To obtain the superoleophilic and superoleophobic surfaces, it is necessary to used substrates with a proper rough structure.[1,17] In this work, copper was chosen as the substrate due to its resistance to corrosion which is important for underwater applications. The nanostructures on the copper substrates were prepared through a simple solution immersion process (the solution is composed of NaOH and $(NH_4)_2S_2O_8$, for more details see the Experimental Section).[38,39] Figure 1 shows the SEM images of the obtained surfaces after immersion in reaction solution for different times. It can be seen that when the immersion time is about 60 s, $Cu(OH)_2$ nanorods with a length of about 3 μm lie on the copper substrate sparsely (see the Supporting Information, Figure S1). As the reaction time is increased to about 120 s (Figure 1b), the nanorods begin grow upwardly and clusters of nanorods would be formed. Increasing the reaction time to about 180 s, more nanorods would be produced, but some areas on the substrate are still exposed (Figure 1c). Further increasing the reaction time to about 300 s (Figure 1d), the whole substrate would be covered by the nanorods completely, and the distribution of the nanorods on the surface becomes much denser. Figure 1e shows the magnified image of the surface, one can find that the diameter of the nanorods is in the range of about 80−150 nm, and the length is about 12 μm (Figure 1f). From the above, it can be concluded that the surface microstructures can be controlled just through varying the immersion time.

To obtain surfaces with controlled wettability, we used two thiols molecules ($HS(CH_2)_9CH_3$ and $HS(CH_2)_{11}OH$, see the Supporting Information, Figures S2−S4) to modify the substrates.[49−51] Figure 2a shows the XPS result of the surface prepared with X_{OH} = 0.6 (X_{OH} is the mole fraction of $HS(CH_2)_{11}OH$ in the modified solution, the reaction time for production of $Cu(OH)_2$ is about 300 s). One can find the elements S, Cu, O, Au, and C on the surface. Panels b and c in Figure 2 are the C 1s high-resolution XPS spectra, from which more information related to the change of surface chemistry can be observed. Compared with the original $Cu(OH)_2$ nanorods surface, one can find that the intensity of C 1s peak at 284.8 eV ascribed to C−C/C−H is increased on the surface modified with single hydrophobic $HS(CH_2)_9CH_3$ (X_{OH} = 0, Figure 2b, a weak peak for the $Cu(OH)_2$ film is due to a little impurity[52]). As the X_{OH} is increased (for example X_{OH} = 0.6, Figure 2c), a new peak at 286.6 eV ascribed to C−O[38] can be observed, indicating that the molecule $HS(CH_2)_{11}OH$ has been assembled on the surface successfully. Meanwhile, it is worth noting that as the X_{OH} is increased, the ratio of C1s peak intensity of C−O to that of the C−C/C−H is increased (Figure 2d), means that more hydroxyl groups can be assembled on the surface. From the above, it can be concluded that the surface composition can be controlled by changing the mole ratio of the two thiols molecules in the modified solution, which would be an important factor for the controllability of the underwater oil wettability on the surfaces.

Through the contact angle measurements, we examined the underwater oil wetting properties of the surfaces. On the surface prepared with X_{OH} = 0.2 (the immersion time for fabrication of $Cu(OH)_2$ is about 300 s), an oil droplet (1,2-dichloroethane, 4 μL) can spread quickly and the surface is underwater superoleophilic with a contact angle of about 0° (Figure 3a) whereas on the surface prepared with X_{OH} = 0.6 (the same microstructures as the above surface), the oil droplet can stand on the surface like a sphere and the contact angle is about 160° (Figure 3b), indicating that the surface is underwater superoleophobic. Furthermore, the surface also shows low adhesion to oil droplet. The advancing/receding

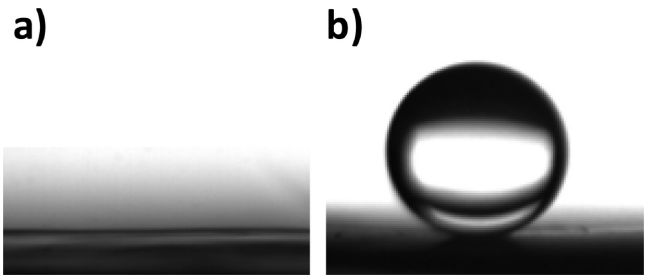

Figure 3. (a) Shape of an oil droplet (1, 2-dichloroethane, 4 μL) on the surface prepared with X_{OH} = 0.2 in water, the contact angle is about 0° and the surface is superoleophilic. (b) Shape of a similar oil droplet on the surface prepared with X_{OH} = 0.6 in water, the contact angle is about 160° and the surface is superoleophobic.

contact angles for the oil droplet on the surface in water are about 162 and 158°, respectively. The contact hysteresis is so small that an oil droplet can roll easily on the surface with a low sliding angle of about 3° (see the Supporting Information, Figure S5). Noticeably, the obtained surfaces can retain the superoleophilicity and superoleophobicity even after 1 week immersion in water, demonstrating the stable superoleophilicity and superoleophobicity in water.

Figure 4 shows the relationship between the underwater oil contact angle and the immersion time for the fabrication of

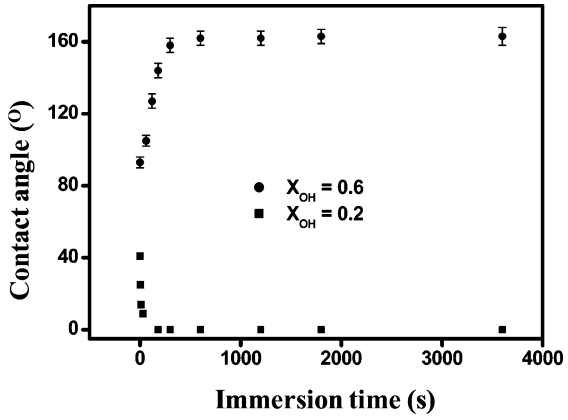

Figure 4. Dependence of oil contact angles on the immersion time for the preparation of $Cu(OH)_2$ nanorods. When the immersion time is larger than 300 s, superoleophilic and superoleophobic performance can be observed on surfaces prepared with X_{OH} = 0.2 and 0.6, respectively.

$Cu(OH)_2$ nanorods. For surfaces prepared with X_{OH} = 0.2 and 0.6, the reverse trend of the variation of contact angles can be seen as the reaction time is increased. When the immersion time is about 300 s, the underwater superoleophilicity and superoleophobicity can be achieved for the surface prepared with X_{OH} = 0.2 and 0.6, respectively. Further increasing the reaction time, the contact angles would level off to the values of about 0 and 163°, respectively (see the Supporting Information, Figure S6). The variation in the oil contact angles is in good agreement with different densities and sizes of the $Cu(OH)_2$ nanorods formed at different immersion times (Figure 1), further confirming that a proper rough structure is very important for the fabrication of superoleophilic and superoleophobic surfaces.

As mentioned above, surface with the same microstructures prepared with different X_{OH} (X_{OH} = 0.2 and 0.6) shows apparently opposite wettability (Figure 3), means that variation of surface chemical composition may also offer a way to control oil wettability on the substrates. Figure 5a shows the

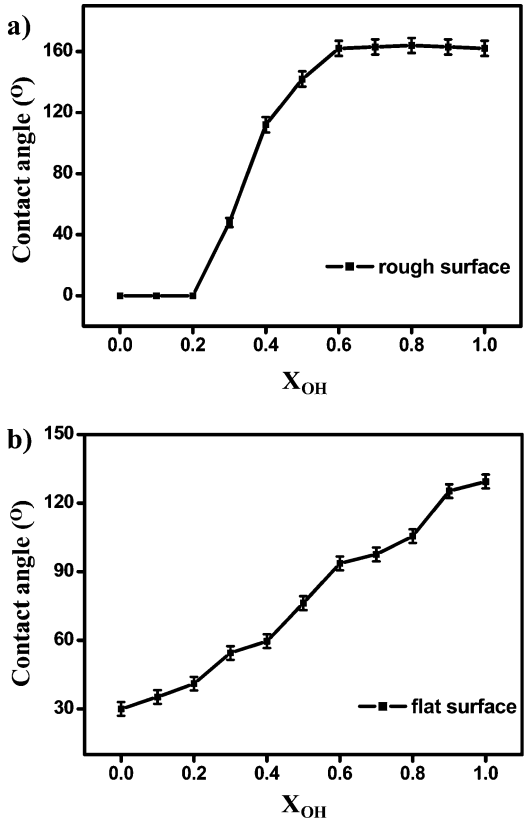

Figure 5. Underwater oil contact angles as a function of the X_{OH} on (a) rough and (b) smooth copper surfaces, respectively.

dependence of oil contact angles on the X_{OH} for rough surfaces (all the surfaces were obtained at the same immersion time at about 300 s). It can be seen that the contact angle increases from about 0° when $X_{OH} \leq 0.2$ to about 163° as the $X_{OH} \geq 0.6$, indicating that the oil wettability on the nanostructured surface can be manipulated to a larger extent by controlling the surface chemical composition. For a comparison, flat copper substrates were modified through the same method. Nevertheless, the variation of the contact angle on the flat surfaces is very limited: from about 30 to 129° (Figure 5b). From the above, it can be found that surfaces with controlled oil wettabilities from underwater superoleophilicity to superoleophobicity can be realized by simply controlling the surfaces chemical composition on the nanostructured substrates. Furthermore, some other oils, such as chloroform, n-hexane and silicon oil were also used to investigate the surface wettability. As shown in Figure 6, the superoleophilic and superoleophobic phenomena can also be observed on surfaces prepared with different X_{OH}, proving that the controllability of our surfaces is universal regardless of the oil type.

To have a better understanding of the oil wettability on the as-prepared surfaces, we carefully analyzed the mechanism affecting the contact angles. In the solid/water/oil three-phase system, the oil contact angle on a flat solid surface can be calculated from the following equation[53,54]

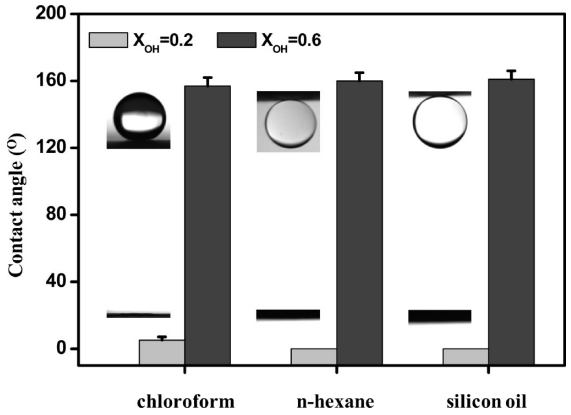

Figure 6. Statistics of the contact angles for different oil droplets on the surfaces prepared with X_{OH} = 0.2 and 0.6, respectively. Insets are the shapes of a corresponding oil droplet on the surfaces. It can be seen that obtained surfaces can show superoleophilicity and superoleophobicity to various oil.

$$\cos\theta_{ow} = \frac{\gamma_{oa}\cos\theta_o - \gamma_{wa}\cos\theta_w}{\gamma_{ow}} \quad (1)$$

where θ_w, θ_o, and θ_{ow} are the contact angles of water in air, oil in air, and oil in water, respectively. γ_{ow}, γ_{wa}, and γ_{oa} are surface tensions of the oil/water, water/air, and oil/air interfaces. In this work, the increase in oil contact angle on the flat surfaces can be ascribed to the variation of surface chemistry as the X_{OH} is increased (Figure 5b). The increase in X_{OH} would increase the amount of the surface hydroxyl groups and strengthen the hydrophilicity of the surface, which means the θ_w would be decreased (see the Supporting Information, Figure S7). As the γ_{oa}, $\gamma_{wa,}$ and γ_{ow} are constant and the θ_o has no evident changes (see the Supporting Information, Figure S8), thus, according to the above equation, the oil contact angle θ_{ow} would be increased as the X_{OH} is increased.[55]

As to rough surfaces, the change tendency of oil contact angle is alike to that on the flat surfaces whereas a remarkable enhanced effect can be observed (Figure 5a). For the surfaces prepared with $X_{OH} \leq 0.2$, the surfaces show underwater superoleophilicity. Recently, Jin et al. reported that the air trapped among the microstructures plays an important role in the surface underwater superoleophilicity: the superoleophilicity is ascribed to the spreading of oil droplet on the air/water interface. As the air is decreased, the surface would transform from the underwater superoleophilicity to the superoleophobicity.[56] In this work, for the surfaces prepared with $X_{OH} \leq 0.2$, the surface are mainly composed of hydrophobic HS-$(CH_2)_9CH_3$ molecules and show superhydrophobicity in air (Figure 7c, see the Supporting Information Figure S9). When these surfaces are immersed into water, a layer of air can also be trapped among the nanostructures (for more details, see the Supporting Information, Figure S10a).[57−60] However, the underwater superoleophilicity of these surfaces cannot be ascribed to the air. Because the $HS(CH_2)_9CH_3$ molecule is hydrophobic/oleophilic, the air would be expelled and the oil would enter into the nanostructures when it contact the surface (see the Supporting Information, Figure S11). In this case, the nanostructures on the surface would enhance the oleophilicity, which can be described by the Wenzel equation.[54,61] On the rough surface, in addition to the $Cu(OH)_2$ nanorods (Figure 1), a layer of gold nanoparticles can also be observed on the nanorods (see Figure S2 in the Supporting Information). Such

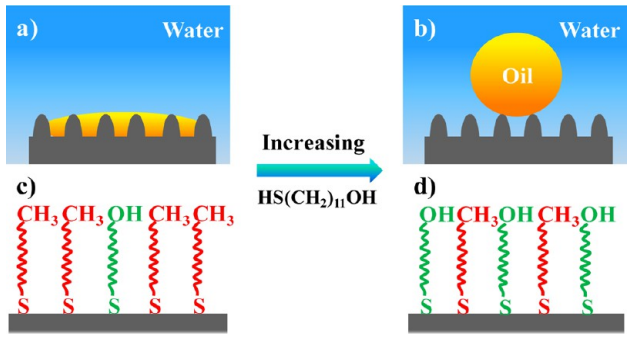

Figure 7. Schematic illustration of underwater oil wettability on the obtained surfaces: for surfaces prepared with $X_{OH} \leq 0.2$, the surfaces are mainly covered by the hydrophobic and oleophilic methyl groups (c), thus the oil droplet can enter into the microstructures and the surface would show underwater superoleophilicity (a). As to the surface prepared with $X_{OH} \geq 0.6$, lots of hydroxyl groups (d) would increase the hydrophilicity of the surface and water can enter into the microstructures; the oil droplet would reside in the composite Cassie state, and the surface would show superoleophobicity (b).

hierarchical structures can increase the surface roughness and the surface area apparently. Thus the inhalation of oil into the rough surfaces can happen because of the three- dimensional capillary effect, and the surface would exhibit underwater superoleophilicity (Figure 7a).

As the X_{OH} is increased, more hydrophilic hydroxyl groups can be assembled on the surfaces. When such surfaces are immersed into water, the hydrogen bonding between water molecules and these hydroxyl groups can be formed[62] and some water can be trapped among the nanostructures. Thus the oil contact angle would be increased because some oil/water interface can be formed instead of the oil/solid interface (Figure 5a). Especially on these surfaces prepared with high X_{OH} ($\geq$ 0.6, Figure 7d), the amount of surfaces hydroxyl groups is high enough that it can lead to the hydrophilicity and even superhydrophilicity of the surfaces (see the Supporting Information, Figure S12). When these surfaces are immersed into water, water can enter into the microstructures easily and occupy the whole interspaces between the nanorods on the surfaces (for more details, see the Supporting Information Figure S10b). As the oil droplet was placed on such surfaces, the oil droplet would reside on a composite solid/water interface (Figure 7b). The high oil contact angles can be explained by the modified Cassie equation[1,63]

$$\cos\theta'_{ow} = f\cos\theta_{ow} + f - 1 \quad (2)$$

where f is the area fraction of the solid contact with oil droplet, θ'_{ow} is the oil contact angle on a rough solid surface in water, and θ_{ow} is the oil contact angle on a flat solid surface in water. Taking the surface prepared with X_{OH} = 0.6 as an example, θ'_{ow} = 160°, θ_{ow} = 94° (Figure 5), and f = 0.065, indicating that more than 93% contact area was water/oil contact area when the oil droplet was dropped on the rough surface. Therefore, the underwater superoleophobic and easy rolling performance can be observed on the surface. Similar reasons can also be suitable to those surfaces prepared with X_{OH} = 0.7, 0.8, 0.9, and 1.0. From the above, one can find that the hierarchical structures composed of $Cu(OH)_2$ nanorods and gold nanoparticles on the surface can enhance the surface wettability to the extremes: underwater superoleophilicity and superoleophobicity. Thus, it would be easy to understand the phenomena displayed in Figure 4, that different oil contact angles can be

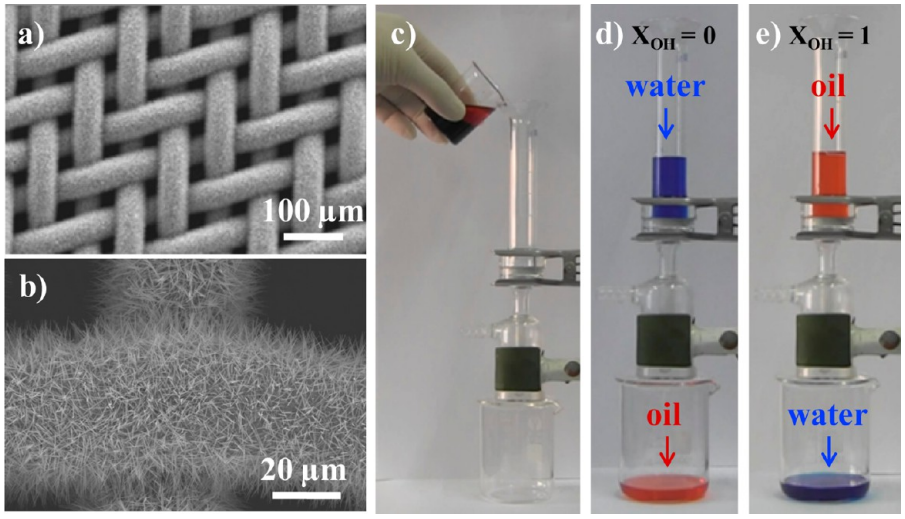

Figure 8. (a, b) SEM images of nanostructured copper mesh film at low and high magnifications; (c) optical photograph of the oil/water separation device; (d) using the film prepared with X_{OH} = 0 as the separating membrane, oil can permeate the film and water can be retained, (e) whereas when the film prepared with X_{OH} = 1 was used, only water can pass through the film, indicating that selective oil/water separation can be realized.

observed as the immersion time is increased. This can be ascribed to the different sizes and densities of nanorods on the surfaces, which may contribute different roughness and ultimately different enhanced effect would be observed.

The strategy reported here is versatile and can be easily extended to some other substrates, for example, copper mesh substrate. Images a and b in Figure 8 show the SEM images of the copper mesh substrate; it can be seen that after immersion into the solution of NaOH and $(NH_4)_2S_2O_8$, nanorods can also be produced on the substrates. After modification with different mixed thiol solution, copper mesh films with similar controlled underwater oil wettability can be prepared. Importantly, such copper mesh films can be used in the oil/water separation, which has aroused much attention in recent years for lots of oil spillage and chemical leakage accidents.[64,65] As shown in Figure 8c, the copper mesh film can be fixed between two glass tubes as the separating membrane. By simply controlling the $HS(CH_2)_{11}OH$ in the modified solution, the obtained copper mesh films have different oil wettabilities. Accordingly, different oil/water separation phenomena can be observed. For films prepared with low X_{OH}, for example, X_{OH} = 0, the film is superhydrophobic and superoleophilic (see the Supporting Information, Figure S13a–c). When the mixture of water and oil (petroleum ether) was poured into the glass tube above the film, only oil can pass through the film and water is retained (Figure 8d, the blue and red color of water and oil for the presence of methylene blue and oil red, respectively). Using the film prepared with high X_{OH}, for example, X_{OH} = 1 (see the Supporting Information, Figure S13d, e), the phenomenon would be just opposite (before the oil/water separation, the film was first wetted by water). Water can permeate the film and oil would be retained (Figure 8e). From the above, it can be found that by simply controlling the $HS(CH_2)_{11}OH$ in the modified solution, oil or water could be selectively separated from the mixture according to one's requirement. We believe such selectively separating membranes can be used in a lot of applications, such as waste water treatment and microfluidic device.

CONCLUSIONS

In summary, a facile approach based on self-assembly of mixed thiols (containing both $HS(CH_2)_9CH_3$ and $HS(CH_2)_{11}OH$) on the nanostructured copper substrates was reported for fabrication of surfaces with controlled oil wettability in water media. By simply changing the concentration of $HS(CH_2)_{11}OH$ in the modified solution, surfaces with controlled oil wettability from the underwater superoleophilicity to superoleophobicity can be achieved. The tunable effect is resulted from the combined effect of the change of surface chemical composition and the microstructures on the surfaces, especially the nanostructures can offer better control of surfaces wettability between the two extremes. Furthermore, the simple concept presented here was also extended to the copper mesh substrates, and selective oil/water separation can be realized on the copper mesh films. We believe that the method reported here may start some new perspectives in manipulating the oil wettability on solid surfaces and have widely applications in, for instance, antipollution, bioadhesive materials, and microfluidic devices.

ASSOCIATED CONTENT

Supporting Information

XRD of $Cu(OH)_2$; SEM images of the surfaces before and after coating with Au; SEM images of surfaces with and without of a layer of Au after reaction with thiol soluction; shape of an oil droplet sliding on the surface prepared with X_{OH} = 0.6 in water; High-resolution Cu 2p XPS spectra of the surfaces; SEM images of surfaces obtained after immersion in reaction soluction for longer time than 300 s; dependence of the water and oil contact angles on the X_{OH} on flat and rough surfaces; optical images of surfaces prepared with X_{OH} = 0.2 and 0.6 underwater before and after contact with oil droplet; shapes of water droplet and oil droplet on copper mesh films prepared with X_{OH} = 0 and 1 in air and water. This material is available free of charge via the Internet at http://pubs.acs.org.

AUTHOR INFORMATION

Corresponding Authors

*E-mail: keningsunhit@163.com. Tel: (+86) 045186412153/ Fax: (+86) 045186412153.
E-mail: znqmww@163.com

Notes

The authors declare no competing financial interest.

ACKNOWLEDGMENTS

This work is supported by the National Natural Science Foundation of China (NSFC Grant 21304025); Open Project of State Key Laboratory of Urban Water Resource and Environment, Harbin Institute of Technology (ES201008); Project (HIT. NSRIF. 2009087) Supported by Natural Scientific Research Innovation Foundation in Harbin Institute of Technology. The Research Fund for the Doctoral Program of Higher Education of china (20112302120062). China Postdoctoral Science Foundation (2011M500650).

REFERENCES

(1) Liu, M.; Wang, S.; Wei, Z.; Song, Y.; Jiang, L. *Adv. Mater.* **2009**, *21*, 665−669.
(2) Liu, X.; Zhou, J.; Xue, Z.; Gao, J.; Meng, J.; Wang, S.; Jiang, L. *Adv. Mater.* **2012**, *24*, 3401−3405.
(3) Xu, L.; Zhao, J.; Su, B.; Liu, X.; Peng, J.; Liu, Y.; Liu, H.; Yang, G.; Jiang, L.; Wen, Y.; Zhang, X.; Wang, S. *Adv. Mater.* **2013**, *25*, 606−611.
(4) Sawai, Y.; Nishimoto, S.; Kameshima, Y.; Fujii, E.; Miyake, M. *Langmuir* **2013**, *29*, 6784−6789.
(5) Xue, B.; Gao, L.; Hou, Y.; Liu, Z.; Jiang, L. *Adv. Mater.* **2013**, *25*, 273−277.
(6) Xue, Z.; Liu, M.; Jiang, L. *J. Polym. Sci., Polym. Phys.* **2012**, *50*, 1209−1224.
(7) Lin, L.; Liu, M.; Chen, L.; Chen, P.; Ma, J.; Han, D.; Jiang, L. *Adv. Mater.* **2010**, *22*, 4826−4830.
(8) Xu, L.; Peng, J.; Liu, Y.; Wen, Y.; Zhang, X.; Jiang, L.; Wang, S. *ACS Nano* **2013**, *7*, 5077−5083.
(9) Chen, L.; Liu, M.; Bai, H.; Chen, P.; Xia, F.; Han, D.; Jiang, L. *J. Am. Chem. Soc.* **2009**, *131*, 10467−10472.
(10) Sheparovych, R.; Motornov, M.; Minko, S. *Adv. Mater.* **2009**, *21*, 1840−1844.
(11) Wischerhoff, E.; Uhlig, K.; Lankenau, A.; Börner, H. G.; Laschewsky, A.; Duschl, C.; Lutz, J.-F. *Angew. Chem., Int. Ed.* **2008**, *47*, 5666−5668.
(12) Truman, P.; Uhlmann, P.; Frenzel, R.; Stamm, M. *Adv. Mater.* **2009**, *21*, 3601−3604.
(13) Ionov, L.; Houbenov, N.; Sidorenko, A.; Stamm, M.; Minko, S. *Adv. Funct. Mater.* **2006**, *16*, 1153−1160.
(14) Wu, D.; Wu, S.; Chen, Q.; Zhao, S.; Zhang, H.; Jiao, J.; Piersol, J. A.; Wang, J.; Sun, H.; Jiang, L. *Lab Chip.* **2011**, *11*, 3873−3879.
(15) Xue, Z.; Wang, S.; Lin, L.; Chen, L.; Liu, M.; Feng, L.; Jiang, L. *Adv. Mater.* **2011**, *23*, 4270−4273.
(16) Tian, D.; Zhang, X.; Tian, Y.; Wu, Y.; Wang, X.; Zhai, J.; Jiang, L. *J. Mater. Chem.* **2012**, *22*, 19652−19657.
(17) Jin, M.; Wang, J.; Yao, X.; Liao, M.; Zhao, Y.; Jiang, L. *Adv. Mater.* **2011**, *23*, 2861−2864.
(18) Yuan, J.; Liu, X.; Akbulut, O.; Hu, J.; Suib, S. L.; Kong, J.; Stellacci, F. *Nat. Nanotechnol.* **2008**, *3*, 332−336.
(19) Zhang, Y.; Wei, S.; Liu, F.; Du, Y.; Liu, S.; Ji, Y.; Yokoi, T.; Tatsumi, T.; Xiao, F. *Nano. Today.* **2009**, *4*, 135−142.
(20) Cheng, M.; Gao, Y.; Guo, X.; Shi, Z.; Chen, J.; Shi, F. *Langmuir* **2011**, *27*, 7371−7375.
(21) Calcagnile, P.; Fragouli, D.; Bayer, I. S.; Anyfantis, G. C.; Martiradonna, L.; Cozzoli, P. D.; Cingolani, R.; Athanassiou, A. *ACS Nano* **2012**, *6*, 5413−5419.
(22) Wang, C.; Tzeng, F.; Chen, H.; Chang, C. *Langmuir* **2012**, *28*, 10015−10019.
(23) Li, S.; Jiao, X.; Yang, H. *Langmuir* **2013**, *29*, 1228−1237.
(24) Deng, D.; Prendergast, D. P.; MacFarlane, J.; Bagatin, R.; Stellacci, F.; Gschwend, P. M. *ACS Appl. Mater. Interfaces* **2013**, *5*, 774−781.
(25) Bi, H.; Xie, X.; Yin, K.; Zhou, Y.; Wan, S.; He, L.; Xu, F.; Banhart, F.; Sun, L.; Ruoff, R. S. *Adv. Funct. Mater.* **2012**, *22*, 4421−4425.
(26) Venkataraman, P.; Tang, J.; Frenkel, E.; McPherson, G. L.; He, J.; Raghavan, S. R.; Kolesnichenko, V.; Bose, A.; John, V. T. *ACS Appl. Mater. Interfaces* **2013**, *5*, 3572−3580.
(27) Wu, J.; Wang, N.; Wang, L.; Dong, H.; Zhao, Y.; Jiang, L. *ACS Appl. Mater. Interfaces* **2012**, *4*, 3207−3212.
(28) Zhu, Q.; Pan, Q.; Liu, F. *J. Phys. Chem. C* **2011**, *115*, 17464−17470.
(29) Guix, M.; Orozco, J.; García, M.; Gao, W.; Sattayasamitsathit, S.; Merkoci, A.; Escarpa, A.; Wang, J. *ACS Nano* **2012**, *6*, 4445−4451.
(30) Cheng, Q.; Li, M.; Yang, F.; Liu, M.; Li, L.; Wang, S.; Jiang, L. *Soft Matter.* **2012**, *8*, 6740−6743.
(31) Huang, Y.; Liu, M.; Wang, J.; Zhou, J.; Wang, L.; Song, Y.; Jiang, L. *Adv. Funct. Mater.* **2011**, *21*, 4436−4441.
(32) Ding, C.; Zhu, Y.; Liu, M.; Feng, L.; Wan, M.; Jiang, L. *Soft Matter* **2012**, *8*, 9064−9068.
(33) Chen, L.; Liu, M.; Lin, L.; Zhang, T.; Ma, J.; Song, Y.; Jiang, L. *Soft Matter* **2010**, *6*, 2708−2712.
(34) Liu, M.; Xue, Z.; Liu, H.; Jiang, L. *Angew. Chem., Int. Ed.* **2012**, *51*, 8348−8351.
(35) Hejazi, V.; Nyong, A. E.; Rohatgi, P. K.; Nosonovsky, M. *Adv. Mater.* **2012**, *24*, 5963−5966.
(36) Liu, M.; Liu, X.; Ding, C.; Wei, Z.; Zhu, Y.; Jiang, L. *Soft Matter.* **2011**, *7*, 4163−4165.
(37) Zhang, L.; Zhang, Z.; Wang, P. *NPG Asia Mater.* **2012**, *4*, e8.
(38) Zhu, X.; Zhang, Z.; Men, X.; Yang, J.; Xu, X. *ACS Appl. Mater. Interfaces* **2010**, *2*, 3636−3641.
(39) Chen, X.; Kong, L.; Dong, D.; Yang, G.; Yu, L.; Chen, J.; Zhang, P. *J. Phys. Chem. C* **2009**, *113*, 5396−5401.
(40) Li, X. M.; Reinhoudt, D.; Crego-Calama, M. *Chem. Soc. Rev.* **2007**, *36*, 1350−1368.
(41) Blossey, R. *Nat. Mater.* **2003**, *2*, 301−306.
(42) Lafuma, A.; Quéré, D. *Nat. Mater.* **2003**, *2*, 457−460.
(43) Roach, P.; Shirtcliffe, N. J.; Newton, M. I. *Soft Matter.* **2008**, *4*, 224−240.
(44) Zhang, X.; Shi, F.; Niu, J.; Jiang, Y.; Wang, Z. *J. Mater. Chem.* **2008**, *18*, 621−633.
(45) Ming, W.; Wu, D.; van Benthem, R.; de With, G. *Nano Lett.* **2005**, *5*, 2298−2301.
(46) Xiu, Y.; Zhu, L.; Hess, D. W.; Wong, C. P. *Nano Lett.* **2007**, *7*, 3388−3393.
(47) Ganesh, V. A.; Raut, H. K.; Nair, A. S.; Ramakrishna, S. *J. Mater. Chem.* **2011**, *21*, 16304−16322.
(48) Hancock, M. J.; Sekeroglu, K.; Demirel, M. C. *Adv. Funct. Mater.* **2012**, *22*, 2223−2234.
(49) Bertilsson, L.; Liedberg, B. *Langmuir* **1993**, *9*, 141−149.
(50) Ulman, A. *Chem. Rev.* **1996**, *96*, 1533−1554.
(51) Yu, Y.; Wang, Z.; Jiang, Y.; Shi, F.; Zhang, X. *Adv. Mater.* **2005**, *17*, 1289−1293.
(52) Wu, X.; Shi, G. *J. Phys. Chem. B* **2006**, *110*, 11247−11252.
(53) Jung, Y. C.; Bhushan, B. *Langmuir* **2009**, *25*, 14165−14173.
(54) Hejazi, V.; Nosonovsky, M. *Langmuir* **2012**, *28*, 2173−2180.
(55) Liu, M.; Nie, F.; Wei, Z.; Song, Y.; Jiang, L. *Langmuir* **2010**, *26*, 3993−3997.
(56) Jin, M.; Li, S.; Wang, J.; Xue, Z.; Liao, M.; Wang, S. *Chem. Commun.* **2012**, *48*, 11745−11747.
(57) Luo, C.; Zheng, H.; Wang, L.; Fang, H.; Hu, J.; Fan, C.; Cao, Y.; Wang, J. *Angew. Chem. Int. Ed.* **2010**, *49*, 9145−9148.
(58) Bobji, M. S.; Kumar, S. V.; Asthana, A.; Govardhan, R. N. *Langmuir* **2009**, *25*, 12120−12126.
(59) Marmur, A. *Langmuir* **2006**, *22*, 1400−1402.
(60) Poetes, R.; Holtzmann, K.; Franze, K.; Steiner, U. *Phys. Rev. Lett.* **2010**, *105*, 166104.

(61) Wenzel, R. N. *Ind. Eng. Chem.* **1936**, *28*, 988−994.
(62) Wang, D.; Liu, Y.; Liu, X.; Zhou, F.; Liu, W.; Xue, Q. *Chem. Commun.* **2009**, 7018.
(63) Cassie, A. B. D.; Baxter, S. *Trans. Faraday Soc.* **1944**, *40*, 546−551.
(64) Zhang, F.; Zhang, W. B.; Shi, Z.; Wang, D.; Jin, J.; Jiang, L. *Adv. Mater.* **2013**, *25*, 4192−4198.
(65) Zhang, X.; Li, Z.; Liu, K.; Jiang, L. *Adv. Funct. Mater.* **2013**, *23*, 2881−2886.